Evidence for Dynamical Dark Energy using DESI DR2 Ly α Forest

Salvatore Capozziello,^{1,2,3,*} Himanshu Chaudhary,^{4,†} G. Mustafa,^{5,‡} and S. K. J. Pacif^{6,7,§}

¹Dipartimento di Fisica "E. Pancini", Università di Napoli "Federico II",

Complesso Universitario di Monte Sant' Angelo, Edificio G, Via Cinthia, I-80126, Napoli, Italy,

²Istituto Nazionale di Fisica Nucleare (INFN), sez. di Napoli, Via Cinthia 9, I-80126 Napoli, Italy,

³Scuola Superiore Meridionale, Largo S. Marcellino, I-80138, Napoli, Italy.

⁴Department of Physics, Babeș-Bolyai University, Kogălniceanu Street, Cluj-Napoca, 400084, Romania

Department of Physics, Zhejiang Normal University, Jinhua 321004, People's Republic of China
 Pacif Institute of Cosmology and Selfology (PICS), Sagara, Sambalpur 768224, Odisha, India
 Research Center of Astrophysics and Cosmology, Khazar University, Baku, 41 Mehseti Street, AZ1096, Azerbaijan

We present a comprehensive analysis of the cosmological implications of the Dark Energy Spectroscopic Instrument (DESI) Data Release 2 (DR2) Lyman-α forest baryon acoustic oscillation (BAO) measurements, combined with complementary datasets DESI DR2 galaxy BAO, Type Ia supernova (Pantheon⁺, DES-SN5Y, and Union3), and compressed CMB likelihood. We test several dynamical dark energy models CPL, logarithmic, exponential, JBP, BA, and GEDE as well as ω CDM and nonflat extensions of the standard Λ CDM and ω CDM models. Using the Metropolis-Hastings MCMC algorithm implemented in SimpleMC, we constrain the cosmological parameters of each model and evaluate the Bayesian evidence using MCEvidence to assess each model's performance relative to Λ CDM. Our results show that the inclusion of DESI DR2 Ly α data modestly enhances sensitivity to departures from ACDM. Our results show non-flat extensions remain consistent with spatial flatness $(\Omega_k \approx 0 \text{ within 1-}2\sigma)$. Further, all redshift-dependent dark energy models predict $\omega_0 > -1$, $\omega_a < 0$, and $\omega_0 + \omega_a < -1$, favor a dynamical dark energy scenario characterized by Quintom-B-type, and we found that dynamical dark energy favors over the Λ CDM model ranging from 0.24–2.60 σ , depending on the choice of model and corresponding combination of datasets. Bayesian evidence comparison favors the ω CDM model with moderate evidence over Λ CDM, whereas other parameterizations remain statistically inconclusive.

I. INTRODUCTION

The accelerated expansion of the Universe remains one of the most profound mysteries in modern cosmology. In the standard Λ CDM paradigm, this acceleration is explained by the cosmological constant Λ , with a constant equation of state parameter $\omega=-1$. However, recent results from the Dark Energy Spectroscopic Instrument (DESI) Data Release 1 (DR1) [1] show deviations from the Λ CDM paradigm at the levels of 2.6σ , 2.5σ , 3.5σ , and 3.9σ when combined with data from the CMB, Pantheon⁺, Union3, and DES Y5, respectively. Furthermore, the more recent DESI Data Release 2 (DR2) [2], when combined with Pantheon⁺, Union3, and DES Y5, reaches deviations of 2.8σ , 3.8σ , and 4.2σ , respectively, strengthening the evidence for a dynamical form of dark energy beyond the simple cosmological constant.

The Lyman- α forest serves as one of the most powerful probes of the high-redshift Universe, providing

precise constraints on the cosmic expansion rate in the range 2 < z < 4 [3, 4]. It arises from a series of absorption features in the spectra of distant quasars, produced by neutral hydrogen in the intergalactic medium (IGM). By analyzing these absorption patterns along numerous lines of sight, the Ly α forest effectively traces the large scale structure of matter at early cosmic times. Over the past decade, surveys such as BOSS, eBOSS, and now DESI have significantly improved measurements of the baryon acoustic oscillation (BAO) scale using both the three dimensional auto correlation of Ly α flux and its cross correlation with quasar positions [3, 5–7]. These studies have demonstrated that the Ly α forest not only provides an independent and robust measurement of the expansion history but also contains additional cosmological information beyond the BAO signal, offering a unique opportunity to test models of dark energy and possible deviations from the Λ CDM paradigm.

Recent results by [8] present cosmological constraints based on the DESI DR1 Ly α forest, providing the first joint measurements that combine the broadband Alcock–Paczynski (AP) and BAO information at high redshift, referred to as the Best-Ly α sample. When combined, the Best-Ly α sample with the Pantheon⁺, Union3, and DES Y5 supernova samples shows prefer-

^{*} capozziello@na.infn.it

[†] himanshu.chaudhary@ubbcluj.ro, himanshuch1729@gmail.com

[‡] gmustafa3828@gmail.com

[§] shibesh.math@gmail.com

ences for a dynamical dark energy model at the 0.8σ , 1.9σ , and 2.1σ levels, respectively. Including CMB data alongside these combinations slightly increases the tension, reaching 1.1σ , 2.0σ , and 2.4σ for the same datasets. The deviation becomes more significant when the Ly α -AP measurements are combined with the CMB, galaxy BAO, and different SNe Ia samples, reaching 2.8σ , 3.8σ , and 4.2σ when adding Pantheon⁺, Union3, and DES Y5, respectively. In addition, the joint Ly α + galaxy BAO + CMB dataset shows a deviation of about 3.1σ , while the combination of Ly α + galaxy BAO alone shows a deviation of about 1.6 σ . These findings align with a growing body of recent studies exploring the implications of DESI observations for new physics in the dark energy sector and potential resolutions to current cosmological tensions. Several recent works have also addressed this issue, aiming to interpret DESI results and others within a broader theoretical framework and to assess whether they point towards extensions of the standard ΛCDM model [9-28].

In this study, we aim to investigate the cosmological implications of the DESI DR2 Lya forest measurements and explore possible deviations from the standard ACDM paradigm. To achieve this, we consider several dark energy (DE) models that allow for a timedependent equation of state and perform a Markov Chain Monte Carlo analysis to constrain the parameter space of each DE model. We also carry out a statistical analysis to test the consistency of these models with the DESI Ly α data. The manuscript is organized as follows. In Section II, we present the mathematical formulation of each DE model. Section III provides a detailed description of the dataset used in this analysis, along with the applied methodology. In Section IV, we discuss our results and their implications in detail. Finally, in Section V, we summarize our main conclusions and outline possible directions for future research.

II. STANDARD COSMOLOGICAL BACKGROUND AND THE Λ CDM FRAMEWORK

General Relativity (GR) forms the cornerstone of modern cosmology and satisfies the criteria established by the Lovelock theorem [29], which states that the Einstein field equations are the only second-order field equations derivable from a scalar density in a four-dimensional spacetime. The gravitational dynamics of the concordance model, ΛCDM, can thus be obtained from the Einstein–Hilbert action, which in natural units

 $(c = \hbar = 1)$ takes the form

$$S = \frac{1}{16\pi G} \int d^4x \sqrt{-g} \left(R - 2\Lambda \right) + S_m, \qquad (1)$$

where Λ is the cosmological constant, $S_m(g_{\mu\nu}, \Psi_m)$ is the action associated with the matter fields Ψ_m , g is the determinant of the spacetime metric $g_{\mu\nu}$, and G is Newton's gravitational constant.

By varying the action (1) with respect to the metric tensor, one obtains the Einstein field equations:

$$R_{\mu\nu} - \frac{1}{2} R g_{\mu\nu} = 8\pi G \left(T_{\mu\nu} - \frac{\Lambda}{8\pi G} g_{\mu\nu} \right), \qquad (2)$$

where $R_{\mu\nu}$ and R are the Ricci tensor and scalar, respectively, and $T_{\mu\nu}$ denotes the energy–momentum tensor. For a perfect fluid,

$$T_{\mu\nu} = (\rho + p)u_{\mu}u_{\nu} + p\,g_{\mu\nu},\tag{3}$$

with ρ and p being the energy density and pressure, and u_{μ} the four-velocity satisfying $u_{\mu}u^{\mu} = -1$.

The Bianchi identities, $\nabla^{\mu}G_{\mu\nu}=0$, together with the Einstein equations, lead to $\nabla^{\mu}T_{\mu\nu}=0$ provided Λ is constant in spacetime. This ensures the local conservation of energy and momentum for all matter fields.

A. Cosmological Dynamics in a Flat FLRW Background

Assuming a homogeneous and isotropic Universe, the spacetime geometry is described by the flat Friedmann–Lemaître–Robertson–Walker (FLRW) metric,

$$ds^{2} = -dt^{2} + a^{2}(t) \left(dr^{2} + r^{2} d\Omega^{2} \right), \tag{4}$$

where a(t) denotes the scale factor and $d\Omega^2 = d\theta^2 + \sin^2\theta \, d\phi^2$. Substituting this metric into Eq. (2) yields the Friedmann equations:

$$3H^2 = 8\pi G \sum_{i} \rho_i,\tag{5}$$

$$2\dot{H} + 3H^2 = -8\pi G \sum_{i}^{i} p_i.$$
 (6)

Here, $H = \dot{a}/a$ is the Hubble parameter, and ρ_i and p_i are the energy density and pressure of the *i*th cosmic component, respectively.

The conservation of the total energy–momentum tensor, $\nabla^{\mu} T_{uv}^{(\text{tot})} = 0$, leads to the continuity equation:

$$\dot{\rho}_i + 3H(1+\omega_i)\rho_i = 0,\tag{7}$$

where $\omega_i = p_i/\rho_i$ is the equation-of-state (EoS) parameter.

For non-relativistic matter ($\omega_m=0$), Eq. (7) gives $\rho_m=\rho_{m0}a^{-3}$, while for dark energy characterized by $\omega_{\rm DE}=-1$, the density remains constant: $\rho_{\rm DE}=\rho_{\rm DE,0}$. Consequently, the dimensionless Hubble function,

$$E(z) \equiv \frac{H^2(z)}{H_0^2},$$

is expressed as

$$E(z) = \Omega_m (1+z)^3 + \Omega_r (1+z)^4 + \Omega_k (1+z)^2 + \Omega_{DE} f_{DE}(z),$$
(8)

where $\Omega_i = (8\pi G \rho_{i0})/(3H_0^2)$ denotes the present density parameter of each component.

B. Dynamical Dark Energy Parameterizations

While the Λ CDM model assumes a constant vacuum energy ($\omega=-1$), theoretical and observational considerations motivate scenarios in which the dark energy equation of state (EoS) varies with time. For a general EoS $\omega(z)$, the dark energy density evolves according to

$$f_{\rm DE}(z) = \exp\left[3\int_0^z \frac{1+\omega(z')}{1+z'} dz'\right].$$
 (9)

If ω is constant, Eq. (9) yields $f_{\rm DE}(z)=(1+z)^{3(1+\omega)}$, i.e., the ω CDM case.

To capture possible time evolution, we consider the following EoS parameterizations:

• Chevallier Polarski Linder (CPL) [30, 31]:

$$\omega(z) = \omega_0 + \omega_a \frac{z}{1+z}.$$

• Logarithmic model [32, 33]:

$$\omega(z) = \omega_0 + \omega_a \ln(1+z).$$

• Exponential model [34–36]:

$$\omega(z) = \omega_0 + \omega_a \left(e^{\frac{z}{1+z}} - 1 \right).$$

• Jassal Bagla Padmanabhan (JBP) [37]:

$$\omega(z) = \omega_0 + \omega_a \frac{z}{(1+z)^2}.$$

• Barboza Alcaniz (BA) [38]:

$$\omega(z) = \omega_0 + \omega_a \frac{z(1+z)}{1+z^2}.$$

• Generalized Emergent Dark Energy (GEDE) [39]:

$$\omega(z) = -1 - rac{\Delta}{3\ln 10} \left[1 + anhigg(\Delta \log_{10}rac{1+z}{1+z_t}igg)
ight]$$
 ,

where Δ and z_t control the transition width and redshift.

Given any $\omega(z)$ above, $f_{DE}(z)$ follows from Eq. (9); inserting this into Eq. (8) yields the corresponding expansion history E(z).

C. Non-flat Universe Extensions

Although the Λ CDM model assumes spatial flatness, several recent analyses suggest that the cosmic curvature may deviate slightly from zero. Planck data indicate a mild preference for a closed Universe [40–42], while low-redshift probes lean towards an open geometry [43]. These tensions motivate considering non-flat cosmologies.

1. Non-flat ΛCDM

Incorporating a curvature component, the dimensionless expansion rate becomes

$$E^{2}(z) = \Omega_{m}(1+z)^{3} + \Omega_{k}(1+z)^{2} + \Omega_{DE}, \quad (10)$$

where Ω_k quantifies the present curvature contribution.

2. Non-flat ωCDM

If dark energy has a constant EoS $\omega \neq -1$, the corresponding expansion rate generalizes to

$$E^{2}(z) = \Omega_{m}(1+z)^{3} + \Omega_{k}(1+z)^{2} + \Omega_{DE}(1+z)^{3(1+\omega)}.$$
(11)

This model highlights the degeneracy between curvature and the dark energy EoS parameter, emphasizing the importance of including Ω_k when constraining cosmic acceleration.

III. DATASET AND METHODOLOGY

We perform the parameter estimation and provide observational constraints on the free parameters of each dark energy model proposed in Section II, and further discuss the implications of these models. To explore the parameter space, we use the Metropolis

Hastings Markov Chain Monte Carlo (MCMC) algorithm [44], integrated with the cosmological inference code SimpleMC [45, 46]. The convergence of the MCMC chains is tested using the Gelman Rubin statistic (R – 1) [47], adopting R-1 < 0.01 as the threshold for convergence. The MCMC results are subsequently analyzed and visualized using the GetDist package [48]. Once the posterior samples are obtained, we compute the Bayesian evidence $\ln \mathcal{Z}$ using MCEvidence [49], which quantifies the compatibility of each statistical model with the observational data. This allows direct comparison between two cosmological models, a and b, through the Bayes factor $B_{ab} \equiv Z_a/Z_b$, or equivalently the relative log-evidence $\ln B_{ab} \equiv \Delta \ln Z$. The model with the smaller $|\ln Z|$ is the preferred one. To interpret the evidence, we use the revised Jeffreys scale [50], where $0 \le |\Delta \ln Z| < 1$ indicates weak evidence, $1 \le |\Delta \ln Z| < 3$ moderate evidence, $3 \le |\Delta \ln Z| < 5$ strong evidence, and $|\Delta \ln Z| \ge 5$ decisive evidence in favor of one model over the other. For parameter estimation, we use the Lyman- α Baryon Acoustic Oscillation (BAO) measurements from the Dark Energy Spectroscopic Instrument (DESI) Data Release 2 (DR2), the galaxy BAO measurements from DR2, Type Ia supernovae, and the compressed CMB likelihood, which are detailed below

- Ly α Forest BAO: We use the Lyman- α (Ly α) forest BAO measurement from the DR2 [51], which provides constraints on the distance ratios $D_{\rm H}(z_{\rm eff})/r_{\rm d}=8.63\pm0.10$ and $D_{\rm M}(z_{\rm eff})/r_{\rm d}=38.98\pm0.53$ at the effective redshift $z_{\rm eff}=2.33$, with a correlation coefficient $\rho=-0.43$.
- **DESI DR2 Galaxy BAO:** In addition to the Ly α forest BAO measurement, we also use the galaxy clustering BAO data from the DESI DR2 [2]. This sample provides measurements of $D_{\rm M}/r_{\rm d}$ and $D_{\rm H}/r_{\rm d}$ in five redshift bins covering the range 0.5 < z < 1.5, as well as a single isotropic BAO constraint at z = 0.295.
- Type Ia Supernovae: We also use the unanchored Type Ia Supernova (SNe Ia) sample from [52], which consists of 1,701 light curves from 1,550 SNe Ia. In our analysis, we exclude supernovae with redshifts z < 0.01 as such low-redshift data are affected by significant systematic uncertainties arising from peculiar velocities. Then, we use the sample of 1,829 photometric light curves collected over five years by the Dark Energy Survey Supernova Program (DES-SN5Y) [53], which includes 1,635 DES-discovered Type Ia supernovae and

194 externally sourced low-z supernovae from the CfA and CSP samples. We also use the **Union3** compilation [54], which contains 2,087 SNe Ia, including 1,363 that overlap with Pantheon⁺, providing complementary redshift coverage. For all supernova datasets, we marginalize over the absolute magnitude parameter \mathcal{M} to account for calibration uncertainties (see Equations A9–A12 in [55]).

• Compressed CMB likelihood: Finally, we use the compressed CMB likelihood because the dynamical dark energy models considered affect only the late-time expansion history of the Universe and mainly modify the geometrical features of the CMB. The full CMB spectrum includes small non-geometrical anomalies, such as the lensing amplitude and the low-\ell power deficit, which may reflect residual systematics and bias dark energy estimates. For example, Planck data alone show a $\gtrsim 2\sigma$ preference for phantom dark energy [56], mostly due to the lack of large-scale power. To avoid such biases, we rely on the compressed CMB likelihood. We use the CMB information compressed into the three parameters $\{R, \ell_a, \omega_b\}$, with $R = \sqrt{\Omega_m H_0^2 D_M(z_*)}$ and $\ell_a = \pi D_M(z_*)/r_s(z_*)$ [57], where $D_M(z_*)$ and $r_s(z_*)$ are the comoving distance and sound horizon at recombination. This 3×3 Gaussian likelihood is known as the Wang-Wang likelihood in SimpleMC.

During our analysis, for each dynamical dark energy model, we assume a spatially flat Universe ($\Omega_k=0$). The present-day radiation density parameter is defined as $\Omega_r=2.469\times 10^{-5}\,h^{-2}\,(1+0.2271\,N_{\rm eff})$, following [58], where $N_{\rm eff}=3.04$ is the standard effective number of relativistic species. The dark energy density parameter is then determined from the flatness condition as $\Omega_{\rm DE}=1-\Omega_r-\Omega_m-\Omega_k$. This ensures a self-consistent reconstruction of both $\Omega_{\rm DE}$ and Ω_r within the assumed flat cosmological framework. This allows both Ω_r and $\Omega_{\rm DE}$ to be fully determined from the other cosmological parameters, rendering them non independent in the parameter estimation. The priors chosen for these models are summarized in Table I.

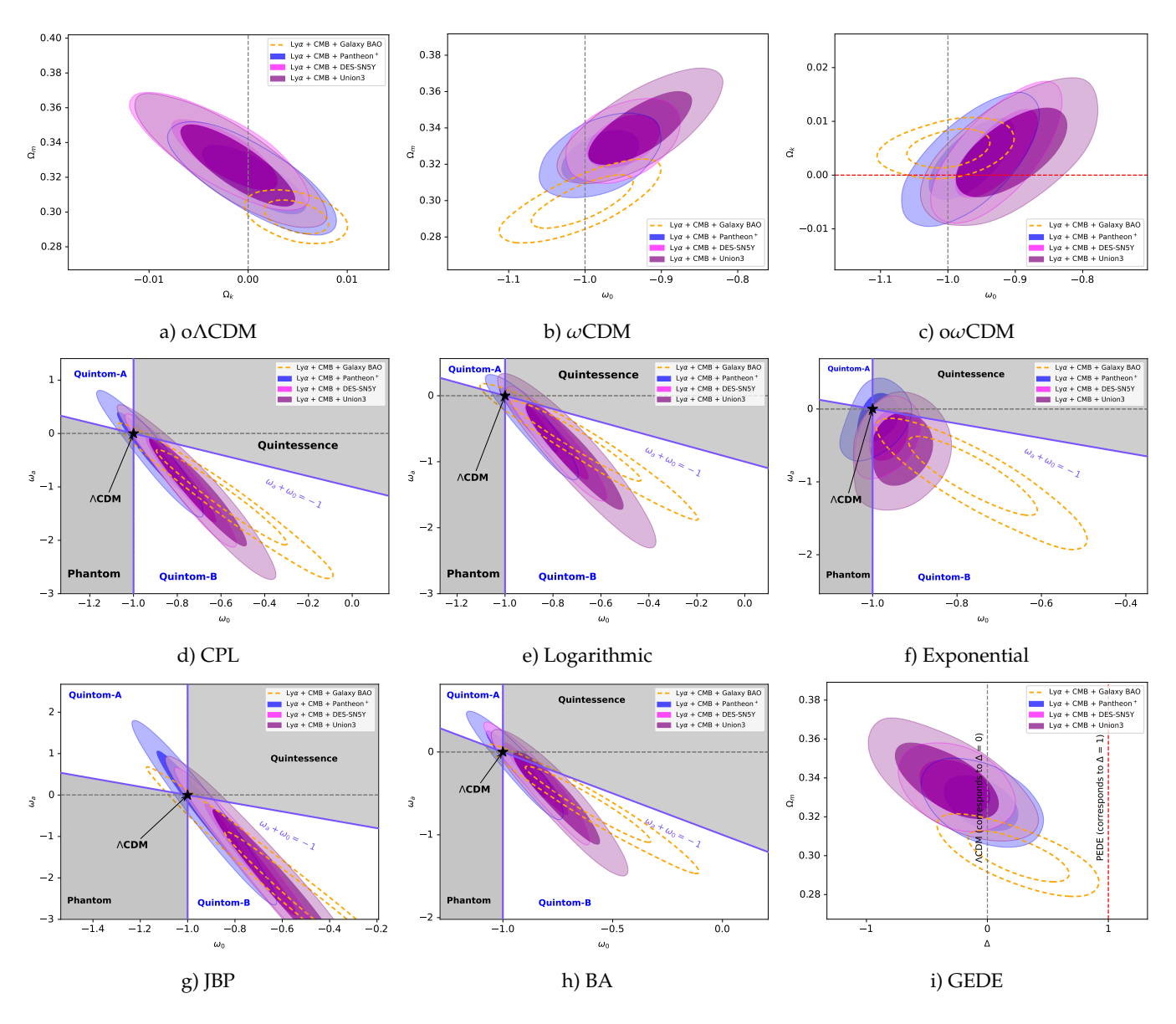


FIG. 1: 2D Posterior distributions of different planes of the o Λ CDM, CPL, $\omega_a\omega_0$ CDM, Logarithmic, Exponential, JBP, BA, and GEDE models using DESI DR2 Lyman- α forest measurements in combination with the CMB, Galaxy BAO, and SNe Ia measurements at the 68% (1 σ) and 95% (2 σ) confidence intervals.

IV. RESULTS

Fig. 1 presents the 2D confidence contours at the 1σ and 2σ levels for the different cosmological models, while Table II shows the mean values of each model's parameters along with their 68% confidence level. In this analysis, we use the parameter values predicted by the Λ CDM model for each combination of datasets, treating it as the baseline model for comparison. In cosmology, we rely on observation based inference, where it is not possible to repeat measurements under identical conditions to achieve the same degree of precision. For

this reason, evidence at the 2–4 σ level is generally considered significant. Several well known anomalies such as the Hubble tension, the S_8 tension, the M_B calibration tension, and the CMB lensing anomaly are discussed as "tensions" precisely because they appear within this range. Therefore, we quantify the deviation of each model parameter from the Λ CDM baseline in terms of the tension (T), defined as $T = \frac{|x_{\rm model} - x_{\Lambda {\rm CDM}}|}{\sqrt{\sigma_{\rm model}^2 + \sigma_{\Lambda {\rm CDM}}^2}}$, where

 $x_{
m model}$ and $x_{
m \Lambda CDM}$ are the predicted parameter values (e.g., h, Ω_m , ω_0), and $\sigma_{
m model}$, $\sigma_{
m \Lambda CDM}$ are their uncertainties. The results are interpreted using the following scale: $|T| < 1\sigma$: consistent with $\Lambda {
m CDM}$; $1\sigma < |T| < 2\sigma$:

Model	Parameter	Prior
ΛCDM	Ω_{m0}	$\mathcal{U}[0,1]$
	$h=H_0/100$	$\mathcal{U}[0,1]$
οΛCDΜ	Ω_{k0}	$\mathcal{U}[-1,1]$
	Ω_{m0} , h	$\mathcal{U}[0,1]$
ω CDM	ω_0	U[-3,1]
	Ω_{m0} , h	$\mathcal{U}[0,1]$
οωCDM	ω_0	U[-3,1]
	Ω_{k0}	$\mathcal{U}[-1,1]$
	Ω_{m0} , h	$\mathcal{U}[0,1]$
	ω_0	U[-3,1]
CPL	ω_a	$\mathcal{U}[-3,2]$
	Ω_{m0} , h	$\mathcal{U}[0,1]$
Logarithmic	ω_0	U[-3,1]
	ω_a	$\mathcal{U}[-3,2]$
	Ω_{m0} , h	$\mathcal{U}[0,1]$
Exponential	ω_0	U[-3,1]
	ω_a	U[-3, 2]
	Ω_{m0} , h	$\mathcal{U}[0,1]$
JBP	ω_0	$\mathcal{U}[-3,1]$
	ω_a	$\mathcal{U}[-3,2]$
	Ω_{m0} , h	$\mathcal{U}[0,1]$
BA	ω_0	U[-3,1]
	ω_a	$\mathcal{U}[-3,2]$
	Ω_{m0} , h	$\mathcal{U}[0,1]$
GDED	Δ	$\mathcal{U}[-10,10]$
	Ω_{m0} , h	$\mathcal{U}[0,1]$

TABLE I: The table shows the parameters and the priors used in our analysis for each DE model. The symbol \mathcal{U} denotes that we use uniform priors, and $h \equiv H_0/100$.

mild tension; $2\sigma < |T| < 3\sigma$: moderate tension; $|T| > 3\sigma$: strong deviation.

First, we compare the predicted values of h for each model with those obtained from the ΛCDM paradigm across different dataset combinations. We find that the level of tension varies depending on both the DE parameterization and the data used. For the Ly α + CMB + Galaxy BAO combination, the exponential model shows a strong deviation from the ΛCDM prediction, while the CPL and BA models exhibit moderate tension. In the case of Ly α + CMB + Pantheon⁺, the CPL model shows moderate tension, and the logarithmic and BA models indicate mild tension. For Ly α + CMB + DES-SN5Y, the exponential model again displays a strong deviation, whereas the JBP and GEDE models show mild tension. For Ly α + CMB + Union3, the CPL and BA parameterizations show moderate tension with respect to the predicted *h* value.

Next, we examine the matter density parameter Ω_m and its deviation from the Λ CDM baseline across the different dataset combinations. The level of tension

again depends on both the DE parameterization and the data used. For the Ly α + CMB + Galaxy BAO combination, the CPL, logarithmic, exponential, and BA models exhibit moderate tension, while the remaining models are in mild tension with Λ CDM. In the case of Ly α + CMB + Pantheon⁺, the logarithmic model shows moderate tension, whereas most other models, including o Λ CDM and o ω CDM, remain consistent or in mild tension. For Ly α + CMB + DES-SN5Y, the CPL and exponential models display moderate tension, while the JBP and GEDE models are consistent with Λ CDM. For Ly α + CMB + Union3, the CPL and BA models show moderate tension, and the other parameterizations remain mildly or fully consistent with Λ CDM.

Now, Figs. 1a, 1b, and 1c show the $\Omega_k - \Omega_m$, $\omega_o \Omega_m$, and $\Omega_k - \omega_o$ confidence contours for the oACDM, ω CDM, and o ω CDM models and present the corresponding constraints on the curvature parameter Ω_k obtained from the various dataset combinations. We find that in the o Λ CDM model, the curvature parameter takes values of $\Omega_k = 0.004 \pm 0.002$ and $\Omega_k = 0.0006 \pm$ 0.0035 for the Ly α + CMB + Galaxy BAO and Ly α + CMB + Pantheon⁺ combinations, respectively. When combined with DES-SN5Y and Union3, the model predicts $\Omega_k = -0.0025^{+0.0038}_{-0.0035}$ and $\Omega_k = -0.0013^{+0.0041}_{-0.0035}$, respectively. Similarly, for the o ω CDM model, all dataset combinations yield $\Omega_k \approx 0$, with values ranging from 0.002 ± 0.005 to 0.005 ± 0.002 . These results are all consistent with zero within $1-2\sigma$ uncertainties. These predictions show close agreement with previous measurements from WMAP ($-0.0179 < \Omega_k < 0.0081, 95\%$ CL) [59], BOOMERanG (0.988 $< \Omega M/R + \Omega_{\Lambda} < 1.0081$, 95% CL) [60], and Planck ($\Omega_{M/R} + \Omega_{\Lambda} = 1.00 \pm 0.026$, 68% CL) [40]. This consistency indicates that all dataset combinations favor a spatially flat Universe.

The ω CDM model predicts $\omega_0 = -1$ when the Ly α data are combined with the CMB and Galaxy BAO, whereas when Ly α is combined with the CMB and different SNe Ia calibrations, it predicts $\omega_0 > -1$. Figs. 1d, 1e, 1f, 1g, and 1h shows the ω_0 – ω_a confidence contour planes for the CPL, Logarithmic, Exponential, JBP, and BA models, respectively. All models predict $\omega_0 > -1$ and $\omega_a < 0$ when the Ly α data are combined with the CMB, different SNe Ia calibrations, and Galaxy BAO, indicating a deviation from the ΛCDM prediction characterized by $(\omega_0 = -1, \omega_a = 0)$. The preferred values of ω_0 and ω_a suggest evidence for a dynamical dark energy scenario, with $\omega_0 > -1$, $\omega_a < 0$, and $\omega_0 + \omega_a <$ −1, consistent with a Quintom-B-type behavior [61, 62]. Fig. 1i shows the Δ - Ω_m confidence contour plane for the GEDE model. We find that the GEDE model predicts $\Delta \approx 0$ when the Ly α data are combined with the CMB

Parameter	Dataset	Λ CDM	oΛCDM	ω CDM	oωCDM	$\omega_a\omega_0$ CDM	Logarithmic	Exponential	JBP	BA	GEDE
h	Lyα + CMB + Galaxy BAO	0.682 ± 0.005	0.694 ± 0.007	0.690 ± 0.011	0.692 ± 0.010	0.651 ± 0.018	0.658 ± 0.020	$0.626^{+0.023}_{-0.021}$	$0.662^{+0.012}_{-0.019}$	0.648 ± 0.020	0.668 ± 0.010
	Lyα + CMB + Pantheon ⁺	0.668 ± 0.006	0.671 ± 0.014	0.664 ± 0.008	0.671 ± 0.014	0.670 ± 0.012	0.671 ± 0.012	0.676 ± 0.012	0.669 ± 0.011	0.671 ± 0.013	0.661 ± 0.008
	Lyα + CMB + DES-SN5Y	0.664 ± 0.006	0.656 ± 0.013	0.655 ± 0.008	0.664 ± 0.014	0.668 ± 0.009	0.673 ± 0.010	0.668 ± 0.009	0.664 ± 0.008	0.668 ± 0.011	$\boldsymbol{0.653 \pm 0.007}$
	Lyα + CMB + Union3	0.666 ± 0.007	0.662 ± 0.016	0.649 ± 0.012	$0.657^{+0.014}_{-0.016}$	0.662 ± 0.012	0.668 ± 0.013	0.664 ± 0.013	0.659 ± 0.012	0.668 ± 0.014	0.650 ± 0.011
Ω_{mo}	Lyα + CMB + Galaxy BAO	0.303 ± 0.006	0.297 ± 0.006	0.299 ± 0.009	0.299 ± 0.008	0.341 ± 0.019	0.333 ± 0.018	$0.369^{+0.031}_{-0.023}$	$0.326^{+0.019}_{-0.014}$	$0.344^{+0.021}_{-0.024}$	0.300 ± 0.008
	Lyα + CMB + Pantheon ⁺	0.321 ± 0.008	0.319 ± 0.013	0.324 ± 0.009	0.318 ± 0.014	0.319 ± 0.012	0.314 ± 0.012	$0.318^{+0.011}_{-0.013}$	0.320 ± 0.011	$0.344^{+0.021}_{-0.024}$ $0.319^{+0.012}_{-0.014}$	0.327 ± 0.009
	Lyα + CMB + DES-SN5Y	0.326 ± 0.008	$0.334^{+0.013}_{-0.014}$	0.332 ± 0.009	0.326 ± 0.014	$0.321^{+0.009}_{-0.011}$	0.317 ± 0.011	0.321 ± 0.010	0.324 ± 0.009	0.322 ± 0.012	0.335 ± 0.009
	Lyα + CMB + Union3	0.323 ± 0.009	$\begin{array}{c} 0.334^{+0.013}_{-0.014} \\ 0.328^{+0.014}_{-0.017} \end{array}$	$0.340^{+0.013}_{-0.014}$	0.332 ± 0.016	0.328 ± 0.013	0.321 ± 0.013	$0.326^{+0.012}_{-0.014}$	$0.330^{+0.012}_{-0.014}$	$0.321^{+0.013}_{-0.014}$	$\boldsymbol{0.338 \pm 0.013}$
Ω_k	Lyα + CMB + Galaxy BAO	_	0.004 ± 0.002	_	0.005 ± 0.002	_	_	_	_	_	
	Lyα + CMB + Pantheon ⁺	_	0.0006 ± 0.0035	_	0.002 ± 0.005	_	_	_	_	_	_
	Lyα + CMB + DES-SN5Y	_	$-0.0025^{+0.0038}_{-0.0035}$	_	0.003 ± 0.005	_	_	_	_	_	_
	Lyα + CMB + Union3	_	$\begin{array}{c} -0.0025^{+0.0038}_{-0.0035} \\ -0.0013^{+0.0041}_{-0.0035} \end{array}$	_	0.004 ± 0.005	_	_	_	_	_	_
ω_0	Lyα + CMB + Galaxy BAO	_	_	-1.004 ± 0.044	$-0.999^{+0.043}_{-0.039}$	-0.547 ± 0.190	-0.690 ± 0.150	$-0.755^{+0.089}_{-0.11}$	$-0.630^{+0.230}_{-0.110}$	$-0.600^{+0.180}_{-0.200}$	_
	Lyα + CMB + Pantheon ⁺	_	_	-0.980 ± 0.033		-0.922 ± 0.098	$-0.895^{+0.072}_{-0.087}$	0.000 ± 0.034	-0.930 ± 0.130	-0.936 ± 0.089	_
	Lyα + CMB + DES-SN5Y	_	_	-0.950 ± 0.031	-0.927 ± 0.040	-0.780 ± 0.100		$-0.990^{+0.030}_{-0.030}$ $-0.964^{+0.033}_{-0.029}$	$-0.750^{+0.140}_{-0.100}$	-0.841 ± 0.097	_
	Lyα + CMB + Union3	_	_	-0.927 ± 0.045	-0.905 ± 0.054		-0.710 ± 0.120	-0.933 ± 0.047	$-0.750^{+0.140}_{-0.100}$ $-0.700^{+0.180}_{-0.100}$	$-0.750^{+0.120}_{-0.140}$	_
ω_a	Lyα + CMB + Galaxy BAO	_	_	_	_	$-1.270^{+0.620}_{-0.540}$	-0.720 ± 0.480	0.050±0.41	$-1.77^{+0.460}_{-1.100}$	$-0.650^{+0.330}_{-0.270}$	_
	Lyα + CMB + Pantheon ⁺	_	_	_	_	$-1.270^{+0.540}_{-0.540}$ $-0.340^{+0.510}_{-0.450}$	$-0.380^{+0.390}_{-0.270}$	$-0.950^{+0.30}_{-0.30}$ $-0.130^{+0.240}_{-0.210}$	-0.360 ± 0.920	-0.150 ± 0.260	_
	Lyα + CMB + DES-SN5Y	_	_	_	_	-0.880 ± 0.520	-0.720 ± 0.350	-0.370 ± 0.230	$-1.43^{+0.770}_{-0.990}$	$-0.340^{+0.310}_{-0.260}$	_
	Lyα + CMB + Union3	_	_	_	_	-1.90 ± 0.650	$-0.920^{+0.550}_{-0.460}$	$-0.560^{+0.360}_{-0.300}$	$-1.580^{+0.580}_{-1.2}$	$\begin{array}{c} -0.340^{+0.310}_{-0.260} \\ -0.550^{+0.410}_{-0.310} \end{array}$	_
Δ	Lyα + CMB + Galaxy BAO	_	_	_	_	_	_	_		_	$0.099^{+0.280}_{-0.320}$
	Lyα + CMB + Pantheon ⁺	_	_	_	_	_	_	_	_	_	-0.05 ± 0.210
	Lyα + CMB + DES-SN5Y	_	_	_	_	_	_	_	_	_	-0.26 ± 0.190
	Lyα + CMB + Union3	_	_	_	_	_	_	_	_	_	-0.32 ± 0.290
$ \Delta \ln \mathcal{Z}_{\Lambda CDM,Model} $	Lyα + CMB + Galaxy BAO	0	2.52	0.62	4.60	2.44	1.69	2.36	2.73	1.86	0.74
	$Ly\alpha + CMB + Pantheon^+$	0	4.54	1.93	6.04	1.91	1.99	2.66	1.25	2.39	0.58
	$Ly\alpha + CMB + DES-SN5Y$	0	4.23	0.67	4.79	0.49	0.02	0.39	1.19	0.37	0.69
	Lyα + CMB + Union3	0	4.44	0.75	3.76	0.91	0.66	0.09	1.45	0.32	0.90
Deviation from ΛCDM	Lyα + CMB + Galaxy BAO	_	_	0.09	0.02	2.38	2.07	2.46	2.18	2.11	0.33
	$Ly\alpha + CMB + Pantheon^+$	_	_	0.61	0.83	0.80	1.32	0.31	0.54	0.72	0.24
	$Ly\alpha + CMB + DES-SN5Y$	_	_	1.61	1.82	2.20	2.60	1.16	2.08	1.64	1.37
	Lyα + CMB + Union3	_	_	1.62	1.76	2.14	2.42	1.43	2.14	1.92	1.10

TABLE II: Numerical values obtained from MCMC analysis for the o Λ CDM, ω CDM, o ω CDM, CPL, Logarithmic, Exponential, JBP, BA, and GEDE models at the 68% (1 σ) confidence level, using DESI DR2 Lyman- α forest measurements in combination with the CMB, Galaxy BAO, and SNe Ia measurements.

and Galaxy BAO, showing close agreement with the Λ CDM model. However, other dataset combinations yield negative values of Δ , indicating a possible injection of dark energy at high redshifts [63, 64]. In terms of deviation, for the Ly α + CMB + Galaxy BAO combination, the $\omega_a\omega_0$ CDM, Logarithmic, Exponential, JBP, and BA models exhibit moderate tension (2.0 σ –2.5 σ), while the ω CDM, o ω CDM, and GEDE models remain consistent with Λ CDM (< 1 σ). For the Ly α + CMB + Pantheon⁺ combination, all models are consistent to mildly tense, with deviations below 1.5 σ . The Ly α + CMB + DES-SN5Y and Ly α + CMB + Union3 combinations show the largest deviations, where the $\omega_a\omega_0$ CDM, Logarithmic, Exponential, JBP, and BA models reach moderate to strong tension (> 2 σ).

Based on the **Bayes** factor differences $|\Delta \ln \mathcal{Z}_{\Lambda CDM,Model}|$ and following the revised Jeffreys scale, we find the following results. For the Ly α + CMB + Galaxy BAO combination, the ω CDM model shows moderate evidence against ΛCDM, while the CPL, Logarithmic, Exponential, JBP, and BA models exhibit weak-to-moderate evidence. The ω CDM and GEDE models remain inconclusive. For the Ly α + CMB + Pantheon⁺ combination, the ω CDM model again shows strong evidence, whereas the CPL, Logarithmic, Exponential, JBP, and BA models provide weak-to-moderate evidence, and ω CDM and GEDE remain inconclusive. In the Ly α + CMB + DES-SN5Y combination, all models yield inconclusive evidence, suggesting comparable performance to Λ CDM. For the Ly α + CMB + Union3 case, the o ω CDM model presents moderate evidence, while most other models show inconclusive to weak evidence.

V. DISCUSSION AND CONCLUSIONS

In this work, we have investigated the cosmological implications of the DESI DR2 Lyman-α forest measurements in combination with several complementary datasets CMB, Galaxy BAO, and multiple Type Ia supernova compilations (Pantheon⁺, DES-SN5Y, and Union3) to test for possible deviations from the standard Λ CDM paradigm. Using a suite of redshift dependent dark energy parameterizations (CPL, Logarithmic, Exponential, JBP, BA, and GEDE) as well as constant EoS and non-flat extensions, we performed a comprehensive Bayesian analysis based on the Metropolis Hastings MCMC algorithm implemented in SimpleMC. Model comparison was carried out via the Bayesian evidence computed using MCEvidence, interpreted through the revised Jeffreys scale. Our main results can be summarized as follows:

• Hubble and Matter Density Parameters: The in-

clusion of DESI DR2 Ly α measurements with other cosmological datasets shows model and data dependent variations in both the Hubble constant h and the matter density parameter Ω_m . In particular, the DESI DR2 Ly α + CMB + Galaxy BAO combination shows the largest deviations from the Λ CDM predictions, with the Exponential model showing strong tension and the CPL and BA models exhibiting moderate tension in h. Similar trends are observed for Ω_m , where several dynamical dark energy parameterizations, including CPL, Logarithmic, Exponential, and BA, show moderate deviation relative to Λ CDM.

• **Spatial Curvature:** The non-flat extensions o Λ CDM and o ω CDM yield curvature constraints consistent with $\Omega_k \approx 0$ within 1–2 σ when the Ly α measurements are combined with other datasets. These findings support the assumption of a spatially flat Universe, in agreement with previous results from WMAP, BOOMERanG, and Planck.

Dynamical Dark Energy Behavior: The inclusion of Lyα data in the combined cosmological analysis favors a dynamical dark energy scenario over the standard ΛCDM framework. Across all redshift-dependent models, the parameter constraints indicate $\omega_0 > -1$, $\omega_a < 0$, and $\omega_0 + \omega_a < -1$, suggesting that dark energy is evolving and characterized by a Quintom-B-type behavior rather than the cosmological constant, where dark energy is characterized by $\omega = -1$. The influence of the Lyα data is particularly evident when combined with the CMB and SNe Ia samples (Union3 and DES-SN5Y), where several models show the deviations from ΛCDM at the 2–3 σ level.

• Bayesian Model Comparison: Including DESI DR2 Ly α data slightly enhances model discrimination, with the o ω CDM model showing moderate tostrong preference over Λ CDM across most combinations. The CPL, Logarithmic, Exponential, JBP, and BA models yield weak to moderate improvements, while ω CDM and GEDE remain statistically consistent with Λ CDM. No model attains decisive evidence.

Our results suggest that when high redshift DESI DR2 Ly α forest measurements are combined with other cos-

mological datasets, the data favor a dynamical dark energy scenario over the cosmological constant. The observed deviations reach the $\sim 2\text{--}3\sigma$ level, which is considered significant given that cosmology relies on observation based inference, where it is not possible to repeat measurements under identical conditions to achieve the same precision. In this context, the $\sim 2\text{--}3\sigma$ evidence provided by the DESI DR2 Ly α forest measurements offers an important hint that the standard ΛCDM model may be entering a phase of increasing tension, revealing potential cracks in the cosmological constant paradigm.

What's next? The upcoming Stage IV surveys will shed new light on the nature of dark energy. DESI will deliver additional DR2 constraints from full-shape fitting, bispectrum, and gravitational lensing in 2025–2026, followed by DR3 BAO results expected in 2027 to provide new insights into the state of dark energy, the ΛCDM model, and the phantom crossing. HST and JWST will refine H_0 , while the Simons Observatory [65], LSST at the Vera C. Rubin Observatory [65], and ESA's Euclid mission [66] will soon provide new CMB, weak lensing, and supernova data. The Subaru PFS survey [67] and the Nancy Grace Roman Space Telescope [68] will extend dark energy constraints beyond z > 1, and DESI-II [69] in the 2030s will push these boundaries even further. If Stage IV surveys challenging the standard Λ CDM model, the next question will be how we move forward. Which new observing methods or cross survey approaches should we focus on first ? Are there particular signals or patterns in the data that could point us towards the true nature of dark energy ? These won't be easy questions to answer. In the long run, we may find that proving Λ CDM is incomplete was the simple part and that understanding what actually drives cosmic acceleration is the much harder task.

ACKNOWLEDGMENTS

SC acknowledges the Istituto Nazionale di Fisica Nucleare (INFN) Sez. di Napoli, Iniziative Specifiche QGSKY and MoonLight-2 and the Istituto Nazionale di Alta Matematica (INdAM), gruppo GNFM, for the support. This paper is based upon work from COST Action CA21136 Addressing observational tensions in cosmology with systematics and fundamental physics (Cosmo-Verse), supported by COST (European Cooperation in Science and Technology).

- 10.1088/1475-7516/2025/02/021.
- [2] M. A. Karim, J. Aguilar, S. Ahlen, S. Alam, L. Allen, C. Allende Prieto, O. Alves, A. Anand, U. Andrade, E. Armengaud, et al., Desi dr2 results ii: Measurements of baryon acoustic oscillations and cosmological constraints, arXiv e-prints (2025) arXiv–2503.
- [3] A. Adame, J. Aguilar, S. Ahlen, S. Alam, D. Alexander, M. Alvarez, O. Alves, A. Anand, U. Andrade, E. Armengaud, et al., Desi 2024 iv: Baryon acoustic oscillations from the lyman alpha forest, Journal of Cosmology and Astroparticle Physics 2025 (01) (2025) 124.
- [4] A. Cuceu, A. Font-Ribera, S. Nadathur, B. Joachimi, P. Martini, Constraints on the cosmic expansion rate at redshift 2.3 from the lyman-*α* forest, Physical Review Letters 130 (19) (2023) 191003.
- [5] T. Delubac, J. Rich, S. Bailey, A. Font-Ribera, D. Kirkby, J.-M. Le Goff, M. M. Pieri, A. Slosar, É. Aubourg, J. E. Bautista, et al., Baryon acoustic oscillations in the $ly\alpha$ forest of boss quasars, Astronomy & Astrophysics 552 (2013) A96.
- [6] A. Slosar, V. Iršič, D. Kirkby, S. Bailey, T. Delubac, J. Rich, É. Aubourg, J. E. Bautista, V. Bhardwaj, M. Blomqvist, et al., Measurement of baryon acoustic oscillations in the lyman-α forest fluctuations in boss data release 9, Journal of Cosmology and Astroparticle Physics 2013 (04) (2013) 026
- [7] H. D. M. Des Bourboux, J. Rich, A. Font-Ribera, V. de Sainte Agathe, J. Farr, T. Etourneau, J.-M. Le Goff, A. Cuceu, C. Balland, J. E. Bautista, et al., The completed sdss-iv extended baryon oscillation spectroscopic survey: baryon acoustic oscillations with $1y\alpha$ forests, The Astrophysical Journal 901 (2) (2020) 153.
- [8] A. Cuceu, H. K. Herrera-Alcantar, C. Gordon, C. Ramírez-Pérez, E. Armengaud, A. Font-Ribera, J. Guy, B. Joachimi, P. Martini, S. Nadathur, et al., Desi dr1 lyα forest: 3d full-shape analysis and cosmological constraints, arXiv preprint arXiv:2509.15308 (2025).
- [9] S. D. Odintsov, V. K. Oikonomou, G. S. Sharov, Dynamical dark energy from F(R) gravity models unifying inflation with dark energy: Confronting the latest observational data, JHEAp 50 (2026) 100471. arXiv:2506.02245, doi:10.1016/j.jheap.2025.100471.
- [10] S. D. Odintsov, D. Sáez-Chillón Gómez, G. S. Sharov, Modified gravity/dynamical dark energy vs ΛCDM: is the game over?, Eur. Phys. J. C 85 (3) (2025) 298. arXiv:2412.09409, doi:10.1140/epjc/ s10052-025-14013-3.
- [11] S. Capozziello, G. Sarracino, A. D. A. M. Spallicci, Questioning the H0 tension via the look-back time, Phys. Dark Univ. 40 (2023) 101201. arXiv:2302.13671, doi:10.1016/j.dark.2023.101201.
- [12] R. C. Bernardo, D. Grandón, J. Said Levi, V. H. Cárdenas, Parametric and nonparametric methods hint dark energy evolution, Phys. Dark Univ. 36 (2022) 101017. arXiv: 2111.08289, doi:10.1016/j.dark.2022.101017.
- [13] E. Di Valentino, et al., The CosmoVerse White Paper: Addressing observational tensions in cosmology with sys-

- tematics and fundamental physics, Phys. Dark Univ. 49 (2025) 101965. arXiv:2504.01669, doi:10.1016/j.dark.2025.101965.
- [14] S. Alam, M. W. Hossain, Beyond cpl: Evidence for dynamical dark energy in three-parameter models, arXiv preprint arXiv:2510.03779 (2025).
- [15] M. van der Westhuizen, D. Figueruelo, R. Thubisi, S. Sahlu, A. Abebe, A. Paliathanasis, Compartmentalization in the dark sector of the universe after desi dr2 bao data, arXiv preprint arXiv:2505.23306 (2025).
- [16] B. R. Dinda, R. Maartens, C. Clarkson, Calibration-independent consistency test of desi dr2 bao and snia, arXiv preprint arXiv:2509.19899 (2025).
- [17] T. Liu, X. Li, T. Xu, M. Biesiada, J. Wang, Torsion cosmology in the light of desi, supernovae and cmb observational constraints, arXiv preprint arXiv:2507.04265 (2025).
- [18] S. R. Choudhury, T. Okumura, Updated cosmological constraints in extended parameter space with planck pr4, desi baryon acoustic oscillations, and supernovae: Dynamical dark energy, neutrino masses, lensing anomaly, and the hubble tension, The Astrophysical Journal Letters 976 (1) (2024) L11.
- [19] S. R. Choudhury, Cosmology in extended parameter space with desi dr2 bao: A 2σ + detection of non-zero neutrino masses with an update on dynamical dark energy and lensing anomaly, arXiv preprint arXiv:2504.15340 (2025).
- [20] S. R. Choudhury, T. Okumura, K. Umetsu, Cosmological constraints on non-phantom dynamical dark energy with desi data release 2 baryon acoustic oscillations: A 3σ + lensing anomaly, arXiv preprint arXiv:2509.26144 (2025).
- [21] S. Lee, Constraining λ cdm, ω cdm, and $\omega_0\omega_a$ cdm models with desi dr2 bao: Redshift-resolved diagnostics and the role of r_d , arXiv preprint arXiv:2507.01380 (2025).
- [22] S. Vagnozzi, New physics in light of the h_0 tension: An alternative view, Physical Review D 102 (2) (2020) 023518.
- [23] J.-Q. Jiang, D. Pedrotti, S. S. da Costa, S. Vagnozzi, Nonparametric late-time expansion history reconstruction and implications for the hubble tension in light of recent desi and type ia supernovae data, Physical Review D 110 (12) (2024) 123519.
- [24] D. Pedrotti, L. A. Escamilla, V. Marra, L. Perivolaropoulos, S. Vagnozzi, Bao miscalibration cannot rescue late-time solutions to the hubble tension, arXiv preprint arXiv:2510.01974 (2025).
- [25] E. Ó. Colgáin, M. M. Sheikh-Jabbari, L. Yin, Can dark energy be dynamical?, Phys. Rev. D 104 (2) (2021) 023510. arXiv:2104.01930, doi:10.1103/PhysRevD.104.023510.
- [26] E. Ó. Colgáin, S. Pourojaghi, M. M. Sheikh-Jabbari, On the Analysis Dependence of DESI Dynamical Dark Energy (5 2025). arXiv: 2505.19029.
- [27] E. Ó. Colgáin, S. Pourojaghi, M. M. Sheikh-Jabbari, L. Yin, How much has DESI dark energy evolved since DR1? (4 2025). arXiv: 2504.04417.
- [28] M. Demianski, E. Piedipalumbo, D. Sawant, L. Amati, High redshift constraints on dark energy models from the

- $E_{p,i}$ E_{iso} correlation in GRBs, Mem. Soc. Ast. It. 89 (2) (2018) 197–204. arXiv:1802.01694.
- [29] D. Lovelock, The einstein tensor and its generalizations, Journal of Mathematical Physics 12 (3) (1971) 498–501.
- [30] M. Chevallier, D. Polarski, Accelerating universes with scaling dark matter, International Journal of Modern Physics D 10 (02) (2001) 213–223.
- [31] E. V. Linder, Exploring the expansion history of the universe, Physical review letters 90 (9) (2003) 091301.
- [32] G. Efstathiou, Constraining the equation of state of the universe from distant type ia supernovae and cosmic microwave background anisotropies, Monthly Notices of the Royal Astronomical Society 310 (3) (1999) 842–850.
- [33] R. Silva, R. Goncalves, J. Alcaniz, H. Silva, Thermodynamics and dark energy, Astronomy & Astrophysics 537 (2012) A11.
- [34] S. Pan, W. Yang, A. Paliathanasis, Imprints of an extended chevallier–polarski–linder parametrization on the large scale of our universe, The European Physical Journal C 80 (3) (2020) 274.
- [35] N. Dimakis, A. Karagiorgos, A. Zampeli, A. Paliathanasis, T. Christodoulakis, P. A. Terzis, General analytic solutions of scalar field cosmology with arbitrary potential, Physical Review D 93 (12) (2016) 123518.
- [36] M. Najafi, S. Pan, E. Di Valentino, J. T. Firouzjaee, Dynamical dark energy confronted with multiple cmb missions, Physics of the Dark Universe 45 (2024) 101539.
- [37] H. Jassal, J. Bagla, T. Padmanabhan, Wmap constraints on low redshift evolution of dark energy, Monthly Notices of the Royal Astronomical Society: Letters 356 (1) (2005) L11–L16.
- [38] E. Barboza Jr, J. Alcaniz, A parametric model for dark energy, Physics Letters B 666 (5) (2008) 415–419.
- [39] X. Li, A. Shafieloo, Evidence for emergent dark energy, The Astrophysical Journal 902 (1) (2020) 58.
- [40] N. Aghanim, et al., Planck 2018 results. vi. cosmological parameters, Astron. Astrophys 641 (2020) A6.
- [41] W. Handley, Curvature tension: evidence for a closed universe, Physical Review D 103 (4) (2021) L041301.
- [42] E. Di Valentino, A. Melchiorri, J. Silk, Planck evidence for a closed universe and a possible crisis for cosmology, Nature Astronomy 4 (2) (2020) 196–203.
- [43] P.-J. Wu, X. Zhang, Measuring cosmic curvature with non-cmb observations, arXiv preprint arXiv:2411.06356 (2024).
- [44] W. K. Hastings, Monte carlo sampling methods using markov chains and their applications (1970).
- [45] J. Vazquez, I. Gomez-Vargas, A. Slosar, Updated version of a simple mcmc code for cosmological parameter estimation where only expansion history matters, https://github.com/ja-vazquez/SimpleMC (2020).
- [46] É. Aubourg, S. Bailey, J. E. Bautista, F. Beutler, V. Bhardwaj, D. Bizyaev, M. Blanton, M. Blomqvist, A. S. Bolton, J. Bovy, et al., Cosmological implications of baryon acoustic oscillation measurements, Physical Review D 92 (12) (2015) 123516. doi:https://doi.org/10.1103/PhysRevD.92.123516.
- [47] A. Gelman, D. B. Rubin, Inference from iterative simu-

- lation using multiple sequences, Statistical science 7 (4) (1992) 457–472.
- [48] A. Lewis, Getdist: a python package for analysing monte carlo samples, Journal of Cosmology and Astroparticle Physics 2025 (08) (2025) 025.
- [49] A. Heavens, Y. Fantaye, A. Mootoovaloo, H. Eggers, Z. Hosenie, S. Kroon, E. Sellentin, Marginal likelihoods from monte carlo markov chains, arXiv preprint arXiv:1704.03472 (2017).
- [50] R. E. Kass, A. E. Raftery, Bayes factors, Journal of the american statistical association 90 (430) (1995) 773–795.
- [51] M. Abdul Karim, J. Aguilar, S. Ahlen, C. Allende Prieto, O. Alves, A. Anand, U. Andrade, E. Armengaud, A. Aviles, S. Bailey, et al., Desi dr2 results. i. baryon acoustic oscillations from the lyman alpha forest, Physical Review D 112 (8) (2025) 083514.
- [52] D. Brout, D. Scolnic, B. Popovic, A. G. Riess, A. Carr, J. Zuntz, R. Kessler, T. M. Davis, S. Hinton, D. Jones, et al., The pantheon+ analysis: cosmological constraints, The Astrophysical Journal 938 (2) (2022) 110.
- [53] T. Abbott, M. Acevedo, M. Aguena, A. Alarcon, S. Allam, O. Alves, A. Amon, F. Andrade-Oliveira, J. Annis, P. Armstrong, et al., The dark energy survey: Cosmology results with 1500 new high-redshift type ia supernovae using the full 5-year dataset, arXiv preprint arXiv:2401.02929 (2024).
- [54] D. Rubin, G. Aldering, M. Betoule, A. Fruchter, X. Huang, A. G. Kim, C. Lidman, E. Linder, S. Perlmutter, P. Ruiz-Lapuente, et al., Union through unity: Cosmology with 2000 sne using a unified bayesian framework, The Astrophysical Journal 986 (2) (2025) 231.
- [55] M. Goliath, R. Amanullah, P. Astier, A. Goobar, R. Pain, Supernovae and the nature of the dark energy, Astronomy & Astrophysics 380 (1) (2001) 6–18.
- [56] L. A. Escamilla, W. Giarè, E. Di Valentino, R. C. Nunes, S. Vagnozzi, The state of the dark energy equation of state circa 2023, Journal of Cosmology and Astroparticle Physics 2024 (05) (2024) 091.
- [57] Y. Wang, P. Mukherjee, Observational constraints on dark energy and cosmic curvature, Physical Review D—Particles, Fields, Gravitation, and Cosmology 76 (10) (2007) 103533.
- [58] E. Komatsu, J. Dunkley, M. Nolta, C. L. Bennett, B. Gold, G. Hinshaw, N. Jarosik, D. Larson, M. Limon, L. Page, et al., Five-year wilkinson microwave anisotropy probe* observations: cosmological interpretation, The Astrophysical Journal Supplement Series 180 (2) (2009) 330.
- [59] G. Hinshaw, J. Weiland, R. Hill, N. Odegard, D. Larson, C. Bennett, J. Dunkley, B. Gold, M. Greason, N. Jarosik, et al., Five-year wilkinson microwave anisotropy probe* observations: data processing, sky maps, and basic results, The Astrophysical Journal Supplement Series 180 (2) (2009) 225.
- [60] P. de Bernardis, P. A. Ade, J. J. Bock, J. Bond, J. Borrill, A. Boscaleri, K. Coble, B. Crill, G. De Gasperis, P. Farese, et al., A flat universe from high-resolution maps of the cosmic microwave background radiation, Nature

- 404 (6781) (2000) 955-959.
- [61] Y. Cai, X. Ren, T. Qiu, M. Li, X. Zhang, The quintom theory of dark energy after desi dr2, arXiv preprint arXiv:2505.24732 (2025).
- [62] G. Ye, M. Martinelli, B. Hu, A. Silvestri, Hints of nonminimally coupled gravity in desi 2024 baryon acoustic oscillation measurements, Physical Review Letters 134 (18) (2025) 181002.
- [63] K. Lodha, A. Shafieloo, R. Calderon, E. Linder, W. Sohn, J. Cervantes-Cota, A. De Mattia, J. García-Bellido, M. Ishak, W. Matthewson, et al., Desi 2024: Constraints on physics-focused aspects of dark energy using desi dr1 bao data, Physical Review D 111 (2) (2025) 023532.
- [64] K. Lodha, R. Calderon, W. Matthewson, A. Shafieloo, M. Ishak, J. Pan, C. Garcia-Quintero, D. Huterer, G. Valogiannis, L. Ureña-López, et al., Extended dark energy analysis using desi dr2 bao measurements, arXiv preprint arXiv:2503.14743 (2025).
- [65] P. Ade, J. Aguirre, Z. Ahmed, S. Aiola, A. Ali, D. Alonso, M. A. Alvarez, K. Arnold, P. Ashton, J. Austermann, et al., The simons observatory: science goals and forecasts, Journal of Cosmology and Astroparticle Physics

- 2019 (02) (2019) 056.
- [66] R. Laureijs, J. Amiaux, S. Arduini, J.-L. Augueres, J. Brinchmann, R. Cole, M. Cropper, C. Dabin, L. Duvet, A. Ealet, et al., Euclid definition study report, arXiv preprint arXiv:1110.3193 (2011).
- [67] M. Takada, R. S. Ellis, M. Chiba, J. E. Greene, H. Aihara, N. Arimoto, K. Bundy, J. Cohen, O. Doré, G. Graves, et al., Extragalactic science, cosmology, and galactic archaeology with the subaru prime focus spectrograph, Publications of the Astronomical Society of Japan 66 (1) (2014) R1.
- [68] D. Spergel, N. Gehrels, C. Baltay, D. Bennett, J. Breckinridge, M. Donahue, A. Dressler, B. S. Gaudi, T. Greene, O. Guyon, et al., Wide-field infrarred survey telescopeastrophysics focused telescope assets wfirst-afta 2015 report, arXiv preprint arXiv:1503.03757 (2015).
- [69] K. Dawson, A. Hearin, K. Heitmann, M. Ishak, J. U. Lange, M. White, R. Zhou, Snowmass2021 cosmic frontier white paper: High density galaxy clustering in the regime of cosmic acceleration, arXiv preprint arXiv:2203.07291 (2022).